To obtain a nontrivial solution, the determinant Δ of the system of the linear equation (4) must equal zero.

For the panel to undergo flutter instability, one has to seek the combination of ω and λ (minimum) that will fulfill Eq. (3) and $\Delta=0$, rendering the system from neutral stability ($\alpha=0$) to instability ($\alpha>0$). The detailed procedure for solving the problem is stated in Ref. 6.

Applications

Assuming $\eta=N_x=\lambda=g_t=0$, the panel flutter problem is reduced to a simply supported beam and thus the natural frequencies are well known. Slowly increasing the dynamic pressure λ of the flow ($\eta=N_x=g_t=0$), one can trace the behavior of, say, the first two frequencies, as shown in Fig. 1. The first two modes approach each other ($\alpha=0$) and, at $\lambda_{cr}L^3/D=343.36$ (known value, see Ref. 7), coalesce to render one mode unstable ($\alpha>0$). The behavior of the natural frequencies vs $\lambda L^3/D$ for a very light damped panel ($\eta=0.001$) are plotted in Fig. 1 (dashed lines). For low dynamic pressure, the modes are damped ($\alpha<0$) and at $\lambda_{cr}L^3/D=134.93$ the first mode becomes unstable ($\alpha>0$). The most striking result deduced from Fig. 1 is the sharp reduction in λ_{cr} for the lightly damped case $\eta=0.001$ compared to the undamped case $\eta=0$ (see Ref. 4). A confirmation of this unexpected reduction in λ_{cr} for the very lightly damped panel case was also obtained by applying a three-mode Galerkin approximation.

These interesting theoretical results were followed by an investigation of the coupling effect between the viscoelastic η and external damping g_t coefficients on the panel flutter instability. Figure 2 represents the critical dynamic pressure $\bar{\lambda}_{cr}(=\lambda L^3/D\pi^4)$ vs η for several values of g_t. The results show the destabilizing effect of the viscoelastic damping η for several values of g_t. Figure 3 displays the variation of $\bar{\lambda}_{cr}$ vs g_t for several values of viscoelastic damping η. It is seen that g_t has a stabilizing effect for all values of η. The results of Figs. 2 and 3 emphasize the strong interaction between the viscoelastic and external (viscous) damping on the panel flutter instability. It should be noted that the three-term Galerkin approximation confirms this finding.

Another course of investigation was to determine if there is a coupling between the damping and the midplane forces exerted on the plate. Figure 4 shows results obtained for $\bar{\lambda}_{cr}$ vs η for a plate subjected to a tension or compression midplane force of $\bar{N}_x(=N_xL^2/D\pi^2)=\pm 3$. Again, it can be seen that viscoelastic damping has a strong destabilizing effect for all values of $\eta\neq 0$.

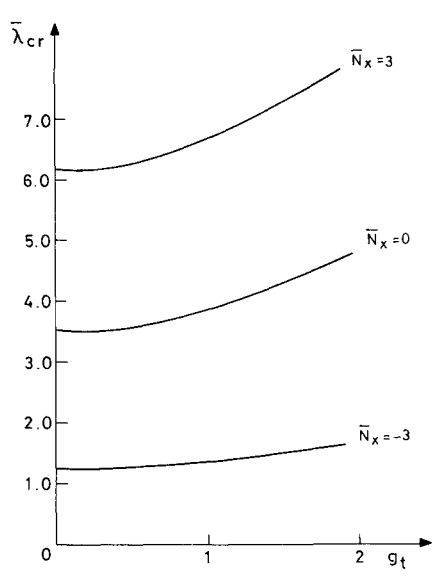

Fig. 5 Variation of the critical dynamic pressure vs external damping for several values of midplane forces.

Figure 5 plots $\bar{\lambda}_{cr}$ vs g_t for several values of the midplane forces while $\eta=0$. g_t has a stabilizing effect on the panel flutter. (The results for $\bar{N}_x=0$ are identical to those obtained in Ref. 8.)

References

[1]Ziegler, H., "Die Stabilitätskriterien der Elastomechanik," *Ingenieur-Archiv*, Vol. 20, No. 1, 1952, pp. 49-56.

[2]Nemat-Nasser, S., Prasad, S. N., and Herrmann, G., "Destabilizing Effect of Velocity-Dependent Forces in Nonconservative Continuous System," *AIAA Journal*, Vol. 4, No. 7, 1966, pp. 1276-1280.

[3]Nemat-Nasser, S. and Herrmann, G., "Some General Considerations Concerning the Destabilizing Effect in Nonconservative Systems," *Zeitschrift fuer Angewandte Mathematik und Physik*, Vol. 17, 1966, pp. 305-313.

[4]Bolotin, V. V. and Zhinzher, N. I., "Effects of Damping on Stability of Elastic Systems Subjected to Nonconservative Forces," *International Journal of Solids and Structures*, Vol. 5, 1969, pp. 965-989.

[5]Bisplinghoff, R. L. and Ashley, H., *Principles of Aeroelasticity*, John Wiley & Sons, New York, 1962, Chap. 8.

[6]Lottati, I. and Kornecki, A., "The Effect of an Elastic Foundation and of Dissipative Forces on the Stability of Fluid-Conveying Pipes," Technion, Haifa, Israel, Rept. TAE No. 563, Feb. 1985.

[7]Hedgepeth, J. M., "Flutter of Rectangular Simply Supported Panels at High Supersonic Speeds," *Journal of the Aeronautical Sciences*, Vol. 24, No. 8, 1957, pp. 563-573.

[8]Houbolt, J. C., "A Study of Several Aerothermoelastic Problems of Aircraft Structures," *Mitteilungen aus dem Institut fur Flugzeugstatik und Leichtbau*, No. 5, E.T.H., Zürich, 1958.

Optimization of Superplastically Formed Sandwich Cores

Charles E. S. Ueng*
Georgia Institute of Technology, Atlanta, Georgia
and
T. David Kim†
Giannoti Associates, Houston, Texas

Introduction

SUPERPLASTIC forming with or without diffusion bonding has proved to be a promising and innovative approach to manufacturing components with complicated shapes in many challenging engineering problems. This new forming process can improve material utilization, simplify machining and assembly, and reduce production costs. It is accomplished through a "one-piece" forming concept that enables the number of parts and fasteners to be greatly reduced. This new technology has been used successfully in different branches of structural engineering, including sophisticated aircraft design, turbine gear manufacture and ground transportation vehicle design. This is confirmed by a recent summary article[1] reporting that more than 200 components in nine current U. S. aircraft and spacecraft (including the B-1B, F-15, F-18A, and Space Shuttle) have been formed superplastically.

Superplastic forming uses a special mechanical property of certain metallic materials that exhibit exceptionally high duc-

Presented as Paper 84-0934 at the AIAA/ASME/ASCE/AHS 25th Structures, Structural Dynamics and Material Conference, Palm Springs, CA, May 14-16, 1984; received Sept. 28, 1984; revision received Nov. 14, 1984.

*Professor, Engineering Science and Mechanics.
†Engineer.

tility under a combination of suitable temperature and strain rate conditions. When in the superplastic state, metal sheets can be deformed readily by ordinary vacuum-forming methods (with an atmospheric or superimposed gas pressure) to gently force the heated metal sheet onto a female die having the complicated geometrical shape desired. This new forming process has been used successfully at Georgia Tech for making different configurations of the cores used in a sandwich composite. Studies have been made on the least-weight design[2,3] and the optimization[4] of a superplastically formed sandwich core.

The mechanical function of the core in such a sandwich composite is to provide sufficient shear rigidity so that there is a very limited shear displacement between the facings when the panel is loaded. A very light sandwich panel lacking the proper shear rigidity is of limited value to an engineer. Conversely, an overweight panel having a high effective shear modulus presents just as many inadequacies. Thus, it is of interest to combine the effects of the two in order to obtain an optimum core design. Furthermore, from a practical viewpoint, the optimized dimensions must be physically achievable in the laboratory. Therefore, suitable constraints on the thickness, spacing, and other dimensions have to be enforced. In this Note, the problem of optimizing the core configuration is investigated with the purpose of maximizing its shear modulus under a number of inequality constraints.

Analysis

The optimization task investigated here is performed through the sequential unconstrained minimization technique (SUMT) developed by Fiacco and McCormick,[5] which utilizes the method of "golden section" searching for optimization. The technique also uses various methods of determining the optimization directions.

The shear modulus of an N-sided, polygonal shaped, truncated, pyramid core geometry with square symmetry having both the upper and lower bound solutions was presented in Ref. 6. In the optimization problem being investigated here, let the function to be maximized, known as the objective function F, be the upper nondimensionalized bound expression of the shear modulus derived in Ref. 6, i.e.,

$$F(\underline{x}) = \frac{G_{\text{eff}}}{G} = \frac{Nt_2(b + d_1 \cos\beta \cot\gamma_N)\sin\beta}{2S^2} \tag{1}$$

where G_{eff} is the effective shear modulus of the core and G the shear modulus of the bulk material from which the core is made. The other terms in Eq. (1) are related to the geometry of the core as shown in Fig. 1 where N is set equal to 8 as an illustration. The constraints needed from manufacturing considerations are

$$\begin{aligned}
g_1(\underline{x}) &= t_1 - t_{\min} \geqq 0 & g_8(\underline{x}) &= a_{\max} - a \geqq 0 \\
g_2(\underline{x}) &= t_{\max} - t_2 \geqq 0 & g_9(\underline{x}) &= b_1 - b_{1\max} \geqq 0 \\
g_3(\underline{x}) &= t_2 - t_{\min} \geqq 0 & g_{10}(\underline{x}) &= b_{1\max} - b_1 \geqq 0 \\
g_4(\underline{x}) &= t_{\max} - t_2 \geqq 0 & g_{11}(\underline{x}) &= d_1 - d_{1\min} \geqq 0 \\
g_5(\underline{x}) &= t_3 - t_{\min} \geqq 0 & g_{12}(\underline{x}) &= d_{1\max} - d_1 \geqq 0 \\
g_6(\underline{x}) &= t_{\max} - t_3 \geqq 0 & g_{13}(\underline{x}) &= \beta - \beta_{\min} \geqq 0 \\
g_7(\underline{x}) &= a - a_{\min} \geqq 0 & g_{14}(\underline{x}) &= \beta_{\max} - \beta \geqq 0
\end{aligned} \tag{2}$$

and from weight consideration

$$G_{15}(\underline{x}) = C - (\rho_{\text{eff}}/\rho) \geqq 0 \tag{3}$$

where ρ_{eff} is the effective core density, ρ the density of the bulk superplastic material, and C the ratio of the two. Thus, the core geometry is sought such that the shear modulus is a maximum for a given core density and the design parameters satisfy the constraint conditions so that the design lies inside a feasible region.

Using the procedure developed by Fiacco and McCormick, a modified objective function is formulated. It consists of the original function F and the penalty functions with the form

$$f = -F - r\sum_{k=1}^{M} \ell n g_k \tag{4}$$

where r is a positive constant and M the number of inequality constraints. The negative sign in front of the objective function converts the shear modulus maximization problem into a minimization one that can be solved by the SUMT method.

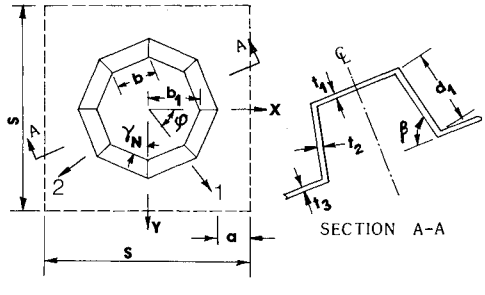

Fig. 1 Unit projection $N=8$.

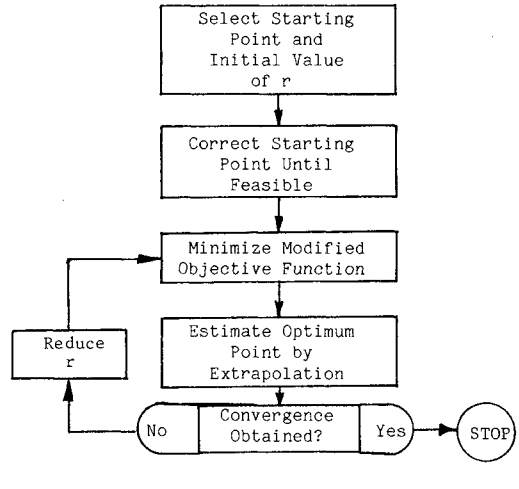

Fig. 2 Logic diagram for SUMT.

Table 1 Optimized shear modulus, $C=0.3$

No. of sides	t_1 (0.2,1)	t_2 (0.2,1)	t_3 (0.2,1)	a (2,5)	b_1 (4,8)	d_1 (5,15)	β (0,90)	ρ_{eff}/ρ (0,0.3)	G_{eff}/G
4	0.33	1.00	0.27	2.00	4.00	12.85	90.00	0.30	0.1374
8	0.67	1.00	0.68	2.00	4.00	10.46	90.00	0.30	0.0744
16	0.70	1.00	0.67	2.00	4.00	10.26	90.00	0.14	0.0379

Note: t_1, t_2, t_3, a, b_1, and d_1 are in millimeters; β in degrees.

Table 2 Optimized shear modulus, $C=0.2$

No. of sides	t_1 (0.2,1)	t_2 (0.2,1)	t_3 (0.2,1)	a (2,5)	b_1 (4,8)	d_1 (5,15)	β (0,90)	ρ_{eff}/ρ (0,0.2)	G_{eff}/G
4	0.20	0.91	0.20	2.00	4.15	15.00	85.91	0.20	0.0943
8	0.59	1.00	0.43	2.00	4.00	11.86	90.00	0.19	0.0744
16	0.69	1.00	0.63	2.00	4.00	10.69	89.99	0.14	0.0379

Note: t_1, t_2, t_3, a, b_1, and d_1 are in millimeters; β in degrees.

Table 3 Optimized shear modulus, $C=0.1$

No. of sides	t_1 (0.2,1)	t_2 (0.2,1)	t_3 (0.2,1)	a (2,5)	b_1 (4,8)	d_1 (5,15)	β (0,90)	ρ_{eff}/ρ (0,0.1)	G_{eff}/G
4	0.20	0.53	0.20	2.00	4.00	15.00	82.09	0.10	0.0448
8	0.20	0.80	0.20	2.00	4.51	15.00	84.77	0.10	0.0439
16	0.49	1.00	0.25	2.00	4.00	13.03	89.99	0.10	0.0379

Note: t_1, t_2, t_3, a, b_1, and d_1 are in millimeters; β in degrees.

Table 4 Optimized shear modulus, $N=4$

C	t_1	t_2 (0.0254,0.254)	t_3	a (2,5)	b_1 (4,8)	d_1 (5,15)	β (0,90)	G_{eff}/G
0.07	0.0254	0.254	0.0254	2.00	4.01	13.8	89.6	0.0341
0.05	0.0254	0.224	0.0254	2.03	4.80	15.0	87.5	0.0242

Note: t_1, t_2, t_3, a, b_1, and d_1 are in millimeters; β in degrees.

The algorithm for the SUMT program proceeds as follows:

1) A modified objective function is formulated as given by Eq. (4). As the algorithm progresses, r is re-evaluated to form a monotonically decreasing sequence $r_1>r_2>\ldots>0$. When r becomes small enough under suitable conditions, f approaches F and the problem is solved.

2) Select a starting point (feasible or nonfeasible) and an initial value for r.

3) Determine the minimum of the modified objective function for the current value of r using an appropriate method such as the Fletcher-Powell in conjunction with the golden section searching technique.

4) Estimate the optimal solution using extrapolation formulas to accelerate the convergence.

5) Select a new value for r and repeat the procedure until the convergence criteria are satisfied.

A logic diagram for this method is given in Fig. 2.

It is not obvious that the solution obtained by the SUMT method is indeed the global maximum. For complex optimization problems such as this, one can only try to optimize with different starting points, either from the feasible or infeasible region, to verify that the same optimum solution is obtained. This is done here and the results are presented in Tables 1-3 for different values of C, the nondimensional effective core density, equal to 0.3, 0.2, and 0.1, respectively. The numbers in parentheses in the tables are the minimum and maximum constraint values for each of the design variables. The last column represents the maximum nondimensional shear rigidity possible under the given constraints.

Discussion and Conclusions

In general, it seems that smaller values of N would provide higher ratios of G_{eff}/G, but at the cost of higher core density. Also, as C decreases, the effective shear rigidity must decrease due to the insufficient amount of material available, with all other constraints being equal. The projection separation distance a remains unchanged at the lower limit for the cases studied, indicating that the maximum shear rigidity is obtained by packing as many projections as possible into a given space. The projection wall thickness t_2 influences the shear modulus directly, as seen from Eq. (1); therefore, the higher values of t_2 correspond to the more rigid cores.

It is interesting to note that for the case $N=16$, i.e., an approximate version of the cone-shaped core, there is no change in the effective shear modulus for different values of C. Comparison of the results in Tables 3 and 2 (or Table 1) for this case indicates that the core may be made lighter by readjusting the geometry without sacrificing its shear rigidity.

In view of the possibility that the thickness of the core could go even thinner than the lower limit used in the computational work as reported in Tables 1-3, two additional runs were made with much lower values for the lower limit of t_1, t_2, and t_3. By the observation mentioned earlier, attention was restricted to the case where $N=4$ only. The value of C was decreased to 0.07 and 0.05. The results are shown in Table 4.

Comparison of the results obtained in this investigation with the available data on the conventional honeycomb core reveals that the maximized effective shear modulus of the core can be considerably more advantageous than the conventional case. For example, pick a honeycomb core made of aluminum foil with a density of 5 lb/ft^3 (80 kg/m^3). This is approximately equal to 3% of the aluminum bulk density (170 lb/ft^3 or 2720 kg/m^3). From p. 28 of Ref. 7, this honeycomb core can provide a shear modulus of about 33 ksi (228×10^6 Pa). Adopting a G value for bulk aluminum to be 3800 ksi (26.2×10^9 Pa), it means that a 3% or 0.03 density ratio can deliver 33/3800 or 0.87% of the bulk shear modulus. On the other hand, for the optimized configuration of a superplastically formed core of 5% or 0.05 density ratio, the value of G_{eff}/G turns out to be equal to 2.42%, a gain by a factor of $(2.42/0.87)(3/5)=1.67$ after the density ratio difference is considered. This is indeed a very promising potential from the study of achieving a high modulus in

such a lightweight structural component. As more superplastic alloys such as 7475 aluminum become commercially available, this type of investigation will undoubtedly attract more attention from the researchers in the area of lightweight structures.

References

[1]Hamilton, C. H., "Superplastic Forming Makes Molded Parts from Sheet Metal Alloys," *Industrial Research and Development*, Vol. 25, Dec. 1983, pp. 72-76.

[2]Ueng, C. E. S. and Liu, T. L., "Least Weight Design of Superplastically Formed Sandwich Cores," *Proceedings of the 2nd ASCE Engineering Mechanics Specialty Conference*, North Carolina State University, Raleigh, May 1977, pp. 440-443.

[3]Ueng, C. E. S. and Liu, T. L., "Least Weight Analysis of a New Sandwich Core," *Proceedings of 14th Annual Meeting of the Society of Engineering Science*, Lehigh University, Bethlehem, Pa., Nov. 1977, pp. 273-283.

[4]Ueng, C. E. S. and Liu, T. L., "Optimization of New Light-Weight Sandwich Core," *Proceedings of International Conference on Light-Weight Shell and Spatial Structures for Normal and Seismic Zones* (sponsored by International Association of Shell and Spatial Structures), Alma-Ata, USSR, Sept. 1977, pp. 375-383.

[5]Fiacco, A. V. and McCormick, G. P., *Nonlinear Programming: Sequential Unconstrained Minimization Techniques*, John Wiley & Sons, New York, 1968.

[6]Ueng, C. E. S. and Kim, T. D., "Shear Modulus of Core Materials with Arbitrary Polygonal Shape," *Computers and Structures*, Vol. 16, No. 1, 1983, pp. 21-25.

[7]"Mechanical Properties of Hexcel Honeycomb Materials," Hexcel Co., Dublin, Calif., Rept. TSB 120, 1974.

Radiative Effect on the Conjugated Forced Convection-Conduction Analysis of Heat Transfer in a Plate Fin

Fue-Sang Lien* and Cha'o-Kuang Chen†
National Cheng Kung University
Tainan, Taiwan, China
and
John W. Cleaver‡
University of Liverpool, Liverpool, England, U.K.

Nomenclature

C_p = specific heat at constant pressure
C_T = temperature difference parameter, $T_\infty/(T_0-T_\infty)$
f = reduced stream function
$h^*,\hat{h}^*$ = dimensional and dimensionless modified heat-transfer coefficients
k,k_f = fluid and fin thermal conductivity
L = fin length
N_c = convection-conduction parameter, $(kL/k_f\delta)Re_L^{1/2}$
N = conduction-radiation parameter, $k\beta^*/4\sigma(T_0-T_\infty)^3$
Pr = Prandtl number, ν/α
q^r = radiative heat flux, $(-4\sigma/3\beta^*)(\partial T^4/\partial y)$, for optically thick limit approximation
Q = overall heat-transfer rate
T,T_f = fluid and fin temperature
T_0 = root temperature
u,v = velocity components in x and y directions, respectively
x,y = coordinates system shown in Fig. 1
α = thermal diffusivity
β^* = extinction coefficient
δ = half-thickness of the fin
ξ,η = pseudosimilarity variables
θ,θ_f = dimensionless fluid and fin temperatures
ν = kinematic viscosity
ρ = density of fluid
σ = Stefan-Boltzmann constant
ψ = stream function

Subscripts

w = condition at wall
∞ = condition at freestream

Received Jan. 23, 1984; revision received Sept. 24, 1984.

*Graduate Student, Department of Mechanical Engineering.
†Professor, Department of Mechanical Engineering.
‡Senior Lecturer, Department of Mechanical Engineering.

Introduction

In the conventional heat transfer analysis of fins, it is standard practice to assume that the heat transfer coefficient for convection at the fin surfaces is uniform. However, there is evidence in the literature demonstrating that the heat-transfer coefficient can experience substantial variations along the fin surfaces.[1,2]

This Note is concerned with fins that transfer heat to a surrounding fluid by forced convection and radiation. The heat-transfer coefficient along the fin is not prescribed, but rather solved in advance from the boundary-layer convection flow. Therefore, the modified local heat transfer coefficient is determined by a highly coupled interaction among the fin conduction, radiation, and fluid convection flow.

The problem to be analyzed here is illustrated in Fig. 1. A vertical fin of length L and thickness 2δ is extended from a wall at temperature T_0 and situated in a uniform freestream having temperature T_∞ and velocity u_∞. The optically thicken limit approximation for the radiative flux is assumed, and the tip for the fin is insulated.

Governing Equations

Consider now a vertical fin parallel to a uniform freestream. Let x and y denote, respectively, the streamwise and normal coordinates. The conservation equations for a laminar boundary layer over a vertical fin is

$$\frac{\partial u}{\partial x}+\frac{\partial v}{\partial y}=0 \tag{1}$$

$$u\frac{\partial u}{\partial x}+v\frac{\partial u}{\partial y}=\nu\frac{\partial^2 u}{\partial y^2} \tag{2}$$

$$u\frac{\partial T}{\partial x}+v\frac{\partial T}{\partial y}=\alpha\frac{\partial^2 T}{\partial y^2}-\frac{1}{\rho C_p}\frac{\partial q^r}{\partial y} \tag{3}$$

subjected to the following boundary conditions:

$$u=v=0,\quad T=T_w,\quad \text{at } y=0$$

$$u=u_\infty,\quad T=T_\infty,\quad \text{as } y\to\infty \tag{4}$$

Introducing pseudosimilarity variables (ξ,η) with a reduced stream function $f(\eta)$ and a dimensionless temperature $\theta(\xi,\eta)$ as

$$\xi=\frac{x}{L},\quad \eta=\left(\frac{y}{L}\right)Re_L^{1/2}/\xi^{1/2},\quad f(\eta)=\psi\frac{(x,y)}{(u_\infty L\xi\nu)^{1/2}},$$

$$\theta=\frac{T-T_\infty}{T_0-T_\infty} \tag{5}$$